ELSEVIER

Biochimica et Biophysica Acta 1341 (1997) 71–78

BIOCHIMICA ET BIOPHYSICA ACTA
BBA

Secondary structure, stability and tetramerisation of recombinant $K_V1.1$ potassium channel cytoplasmic N-terminal fragment

Geoffrey W. Abbott [a], Michael Bloemendal [b], Ivo H.M. Van Stokkum [b], Eric A.J. Mercer [a], Rob T. Miller [c], Sabine Sewing [d], Mark Wolters [d], Olaf Pongs [d], Surjit K.S. Srai [a,*]

[a] *Department of Biochemistry and Molecular Biology, Royal Free Hospital School of Medicine, London, UK*
[b] *Faculty of Physics and Astronomy, Free University, Amsterdam, The Netherlands*
[c] *Biomolecular Structure and Modelling Unit, Department of Biochemistry and Molecular Biology, University College, London, UK*
[d] *Zentrum fur Molekulare Neurobiologie, Institut fur Neurale Signalverarbeitung, Hamburg, Germany*

Received 24 January 1997; revised 1 April 1997; accepted 3 April 1997

Abstract

The recombinant N-terminal fragment (amino acids 14-162) of a tetrameric voltage-gated potassium channel ($K_V1.1$) has been studied using spectroscopic techniques. Evidence is presented that it forms a tetramer in aqueous solution, whereas when solubilised in 1% Triton X-100 it remains monomeric. The secondary structure content of both monomeric and tetrameric $K_V1.1$ N-terminal fragment has been estimated from FTIR and CD spectroscopy to be 20–25% α-helix, 20–25% β-sheet, 20% turns and 30–40% random coil. Solubilisation of the protein in detergent is shown by hydrogen-deuterium exchange analysis to alter tertiary structure rather than secondary structure and this may be the determining factor in tetramerisation ability. Using molecular modelling we propose a supersecondary structure consisting of two structural domains. © 1997 Elsevier Science B.V.

Keywords: Fourier transform infrared spectroscopy; Circular dichroism spectroscopy; Secondary structure; Tertiary structure; Thermal stability; Tetramerisation

1. Introduction

Voltage-gated potassium (K_V) channels consist of four α-subunits arranged symmetrically around an aqueous pore, each subunit consisting of 6 membrane-spanning α-helices (S1-S6), a putative ion selectivity filter (H5) and cytoplasmic N- and C-terminal regions [1,2].

The molecular recognition sequences involved in the subfamily-specific assembly of K_V channel α-subunits are postulated to lie within the A and B subdomains of the T1 domain in the N-terminal region of these proteins (Fig. 5a) [3,4]. N-terminal fragments from K_V1, K_V2, K_V3 and K_V4 subfamilies can all form stable homomultimers [5] and subfamily-specific heteromultimers, and Pfaffinger and

Abbreviations: AA, amino acids; CMC, critical micellisation concentration; DTT, dithiothreitol; FTIR, Fourier-transform infrared; GST, glutathione-S transferase; LB, Luria-Bertani; MBpAB, chain B of mannose-binding protein A; STE, sodium chloride/Tris/EDTA; UV, ultra-violet

* Corresponding author. Fax: +44 171 794 9645. E-mail: sraihsm.ac.uk

PII S0167-4838(97)00062-9

DeRubeis [6] have demonstrated that the *Shaker* T1 domain alone can self-tetramerise to a stable structure, yet Babila et al. [7] claim that S1, the first membrane-spanning domain, together with the T1 domain is necessary for tetramerisation.

In this study we describe the secondary structure content, thermal stability and co-assembly of the $K_V1.1$ α-subunit N-terminal region. Evidence is presented that the recombinant N-terminal fragment in aqueous buffer tetramerises in the absence of the S1 membrane-spanning domain, while in the presence of Triton X-100 it remains monomeric. Using Fourier-transform infrared (FTIR) spectroscopy combined with global analysis [8] and circular-dichroism (CD) spectroscopy, we compare the structure and stability of the tetramerised recombinant $K_V1.1$ N-terminal fragment with that of the monomeric form. We postulate a supersecondary structure model of $K_V1.1$ N-terminal fragment based on computer-predicted models and relate this to our experimental findings.

2. Materials and methods

2.1. Cloning, expression and isolation of $K_V1.1$ N-terminal fragment

Cloning, expression and isolation of pure, recombinant $K_V1.1$ N-terminal fragment were performed as previously described [9].

2.2. Multimerisation of N-terminal fragment in the presence and absence of detergent

Recombinant $K_V1.1$ N-terminal fragment (initial concentration of 1 mg/ml) was applied to 5%–15% linear sucrose-gradients in PBS buffer (150 mM NaCl, 16 mM Na_2HPO_4, 4 mM NaH_2PO_4; pH 7.4) with and without 1% Triton X-100 (v/v). After centrifugation at 55 000 rpm for 20 h at 4°C in an SW28 rotor and a Beckmann XL-80 ultracentrifuge alongside proteins of known molecular mass, 100 μl fractions were collected and analysed for presence of protein using the Bradford assay and SDS-PAGE analysis. Apparent molecular mass of the N-terminal fragment in the presence and absence of Triton X-100 was calculated from sucrose gradient centrifugation results by the method of Martin and Ames [10].

2.3. Fourier-transform infrared (FTIR) spectroscopy

FTIR spectra of $K_V1.1$ N-terminal fragment at 50 mg/ml in PBS/H_2O and PBS/D_2O in the presence and absence of 1% Triton X-100 (v/v) were recorded using a Perkin-Elmer 1750 FTIR spectrometer equipped with a fast recovery TGS detector. Double-sided interferograms were recorded and apodized using a raised cosine function prior to transformation of the data. The programs IRDM (*Perkin Elmer*) and GRAMS (*Galactic*) were used for data handling. Buffer spectra were recorded under identical conditions and subtracted digitally to give a straight baseline in the 2100–1800 cm^{-1} region. Deconvolution of spectra was performed using GRAMS Deconvolve (FSD) function. Typically a full width at half height of 16 cm^{-1} and a Gamma factor of 3.5 were used with 70% Bessel smoothing. Second-derivative spectra were calculated using GRAMS Derivative function with a 13 data point Savitzky-Golay smoothing window. Secondary structure was calculated from the amide I band (1700–1600 cm^{-1}) at 20°C in H_2O by means of a multivariate model [11].

For hydrogen-deuterium exchange measurements, protein samples solubilised in PBS/D_2O in the presence and absence of 1% Triton X-100 (v/v) were kept at 20°C, and spectra (each 100 scans, signal averaged) recorded at progressively greater time intervals from 1 minute to 1 week after buffer addition. Hydrogen-deuterium exchange was also measured as a function of temperature in the detergent-solubilised protein.

For protein-stability measurements, temperature was varied from 20°C to 80°C with a heating rate of 0.13°C/min. For each temperature point 100 scans were signal averaged at a resolution of 4 cm^{-1}. This resulted in measurements every 2°C. Temperature-dependent FTIR data were quantified by global analysis [8,12].

2.4. Circular dichroism (CD) spectroscopy

Far-UV CD spectra (185–260 nm) of 0.4 mg/ml $K_V1.1$ N-terminal fragment in 100 mM sodium phosphate (16 mM Na_2HPO_4, 4 mM NaH_2PO_4, pH 7.4) were recorded at 20°C in a 0.02 cm path-length cell using a Jasco J-600 spectropolarimeter. The instrument was continuously purged with nitrogen to pre-

vent ozone build-up. Secondary-structure content was predicted using the locally-linearized model [13].

2.5. Structure prediction based on amino acid sequence

The N-terminal sequence of $K_V1.1$ was subjected to computerized structure prediction by THREADER program [14].

3. Results

3.1. Multimerisation of N-terminal fragment in the presence and absence of detergent

In the absence of Triton X-100 the N-terminal fragment sedimented to a sucrose density of 10.2%

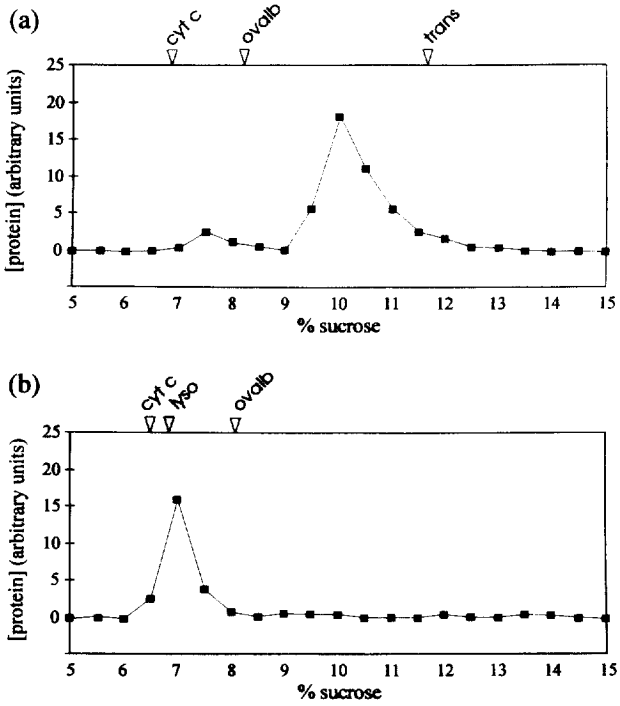

Fig. 1. Effect of Triton X-100 on ability of $K_V1.1$ N-terminal fragment to self-assemble into tetramers. Concentrations of $K_V1.1$ N-terminal fragment at various sucrose percentages after sucrose-gradient sedimentation are shown in relation to migration distances of marker proteins of known mass sedimented on similar sucrose-gradients. Markers shown: cytochrome C (12 kDa), lysozyme (17.2 kDa), ovalbumin (46 kDa) and transferrin (85 kDa). (a) representative sedimentation pattern of $K_V1.1$ N-terminal fragment in PBS buffer without detergent in a 5%–15% linear sucrose-gradient. (b) representative sedimentation pattern of $K_V1.1$ N-terminal fragment in PBS buffer with 1% Triton X-100 detergent (v/v) in a 5%–15% linear sucrose-gradient.

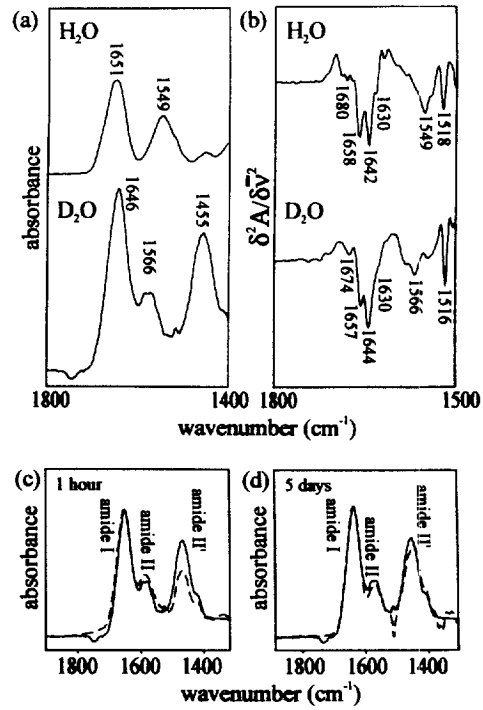

Fig. 2. FTIR analysis of $K_V1.1$ N-terminal fragment. (a) FTIR-absorbance spectra and (b) second derivative spectra of recombinant tetrameric $K_V1.1$ N-terminal fragment in PBS at 20°C: H_2O (top) and D_2O (bottom). (c,d) FTIR absorbance spectra of D_2O PBS-solubilised tetrameric $K_V1.1$ N-terminal fragment (solid line spectra) and monomeric $K_V1.1$ N-terminal fragment in D_2O PBS with 1% Triton X-100 (dashed line spectra). The spectra show extent of hydrogen-deuterium exchange of the monomeric protein after (c) 1 h and (d) 5 days, compared to the essentially complete exchange observed in the tetrameric form after 1 h (c,d).

which corresponded to an apparent molecular mass of 70 kDa, i.e., the fragment had tetramerised (Fig. 1a). In the presence of 1% Triton X-100 (v/v) the protein sedimented to a sucrose density of 7.1% which corresponded to an apparent molecular mass of 18 kDa, i.e., the fragment had remained in monomeric form (Fig. 1b).

3.2. FTIR spectroscopy

3.2.1. $K_V1.1$ N-terminal fragment in aqueous solution (tetrameric form)

3.2.1.1. Secondary structure. The FTIR-absorbance spectra of $K_V1.1$ N-terminal fragment in H_2O and D_2O at 20°C are shown in Fig. 2a. The amide I maxima lie at 1651 cm^{-1} and 1646 cm^{-1}, respectively.

Qualitative information on the secondary structure of a protein can be obtained from an analysis of its amide I band using derivative techniques [15]. The second-derivative spectra (Fig. 2b) show bands at 1680/1674 cm^{-1} (turns), 1658/1657 cm^{-1} (α-helix), 1642/1644 cm^{-1} (random coil), 1549/1566 (amide II and carboxylate) and 1518/1516 cm^{-1} (tyrosine). There is a shoulder at 1630 cm^{-1} in both spectra which can be assigned to β-structures. Prediction of the secondary structure from the spectrum in H_2O yielded $22 \pm 12\%$ α-helix, $25 \pm 8\%$ β-sheet (essentially anti-parallel), $22 \pm 7\%$ turn and $35 \pm 11\%$ other structure.

3.2.1.2. Unfolding and aggregation. Original FTIR spectra of the $K_V1.1$ N-terminal fragment (not shown) between 1400 and 1800 cm^{-1} in D_2O at temperatures between 20°C and 80°C were analysed by global analysis in order to quantify denaturation properties of the fragment. Band intensities plotted against temperature are shown in Fig. 3. The bands attributed to the main secondary structural elements (α-helix 1651 cm^{-1}, 1634 cm^{-1} β-sheet) reduce in intensity simultaneously. Global analysis with a two-state model of these transitions, which represent the thermal unfolding of the protein, gave a midpoint temperature of 46 ± 1°C and a related Van 't Hoff enthalpy of 323 ± 16 kJ/mol. Concomitant with this, a band attributed to aggregated structures that result from thermal denaturation of proteins (1622 cm^{-1}) appears in the spectra. This transition has a midpoint temperature of 45 ± 1°C. Bands at 1523 cm^{-1}, 1571 cm^{-1} (tyrosine and carboxylate, respectively) and 1680 cm^{-1} (turns) show negligible temperature dependence. We are not yet able to interpret the temperature dependence of the 1442 cm^{-1} and 1480 cm^{-1} bands, which are due to side chains as well as to the amide II′ vibration, but temperature-induced band shifts cannot be excluded.

3.2.1.3. Hydrogen-deuterium exchange. The band at 1549 cm^{-1} in H_2O is the amide II band (Fig. 2a). As it is almost absent in D_2O it can be concluded that most of the protons are exchanged by deuterium, and this is reflected by the dominating amide II′ (amide II with ND instead of NH) band at 1455 cm^{-1} (Fig. 2a). In fact, spectra of the protein in D_2O at 20°C recorded as little as 5 min after buffer addition show little or no differences to spectra recorded 1 week after buffer addition. This being the case, it was not possible to study the hydrogen-deuterium exchange of the tetrameric form of the protein as a function of temperature.

3.2.2. $K_V1.1$ N-terminal fragment in aqueous solution with 1% Triton X-100 (v/v) (monomeric form)

3.2.2.1. Secondary structure. Buffer-subtracted FTIR spectra of the monomeric N-terminal fragment solubilised with 1% Triton X-100 (v/v) in H_2O buffer were not significantly different to spectra of the protein in the absence of the detergent, indicating that the Triton X-100 did not significantly affect the secondary structure of the protein.

3.2.2.2. Unfolding and aggregation. Global analysis of the temperature-resolved spectra indicated that the midpoint temperatures of unfolding and aggregation of the protein were similar to those seen without detergent (45–50°C). The Van 't Hoff enthalpy of unfolding was reduced by a factor of four to 77 ± 4 kJ/mol in D_2O (compared to 323 ± 16 kJ/mol without detergent).

3.2.2.3. Hydrogen-deuterium exchange. FTIR spectra of the detergent-solubilised protein in D_2O buffer (Fig. 2c,d) were significantly different to spectra of the protein in the absence of detergent. Hydrogen-deuterium exchange, reflected by an increase in the

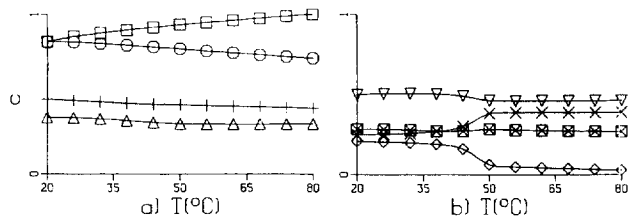

Fig. 3. Thermal stability of tetrameric $K_V1.1$ N-terminal fragment. Temperature-dependent intensity (c) of bands in the absorbance spectra of $K_V1.1$ N-terminal fragment in PBS pH 7.4, plotted against temperature (T). Global analysis of the original FTIR spectra between 1400 cm^{-1} and 1800 cm^{-1} in D_2O PBS at temperatures between 20°C and 80°C yielded bands as follows: (a) 1442 (□) and 1480 (○) (side chains and amide II′); 1523 (Δ) and 1571 (+) (tyrosine and carboxylate respectively); (b) 1622 (X, non-specific aggregation); 1634 (◇, β-sheet); 1651 (▽,_α-helix) and 1680 cm^{-1} (□, turns).

intensity of the amide II′ band and a corresponding decrease in the intensity of the amide II band, occurs more slowly in the Triton X-100-solubilised N-terminal region than it does in the absence of Triton X-100. Indeed it takes several days for exchange in the Triton X-100-solubilised protein to occur to a similar extent to that seen within one hour in the absence of detergent (Fig. 2c,d). This reflects alterations in the tertiary structure of the protein when in the presence of the detergent, compared to when in the absence of detergent.

Because of the slower hydrogen-deuterium exchange observed in the monomeric form of the protein, it was possible to study the rate of exchange as a function of temperature. Global analysis (not shown) of exchange with the protein heated as for the unfolding studies indicated a midpoint temperature of exchange of 41.6 ± 0.8°C, the amide II band in particular showing a sigmoidal decrease with increased temperature.

3.3. CD spectroscopy of $K_v1.1$ N-terminal fragment in aqueous solution (tetrameric form)

The CD spectrum of $K_V1.1$ N-terminal fragment in aqueous solution at 20°C in the region 185–260 nm (Fig. 4) has a minimum at 208 nm with shoulders at 198 nm and around 220 nm. The locally-linearized model gives a secondary-structure prediction of 24 ± 2% helix, 22 ± 7% sheet (essentially anti-parallel), 20 ± 4% turns and 34 ± 6% other structures.

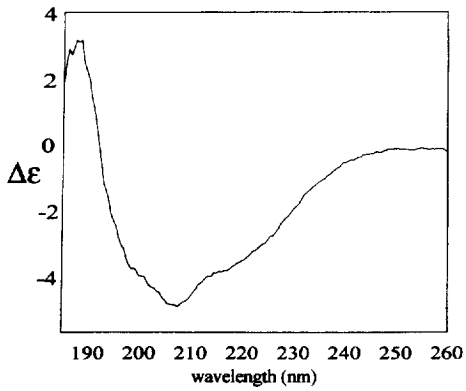

Fig. 4. CD analysis of $K_V1.1$ N-terminal fragment. CD spectrum of $K_V1.1$ N-terminal fragment at 20°C in 100 mM phosphate buffer (pH 7.4).

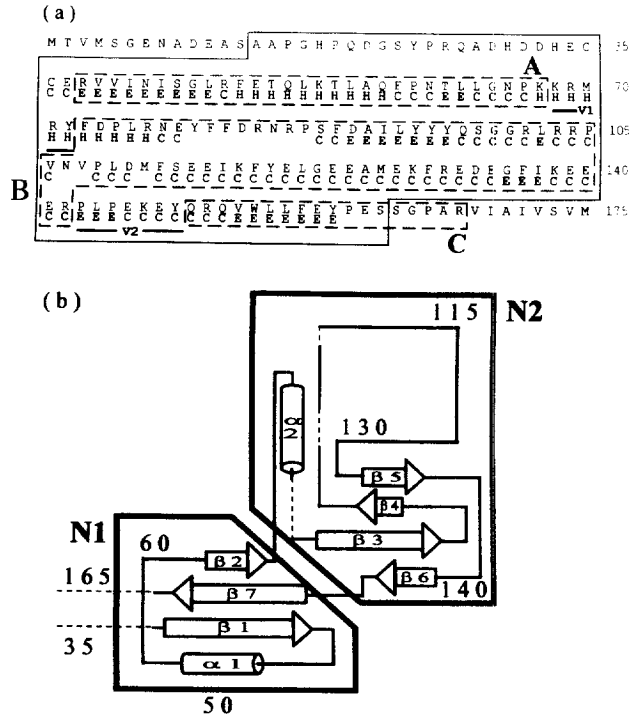

Fig. 5. Functional and structural domains of $K_V1.1$ N-terminal fragment. (a) Amino acid sequence of $K_V1.1$ N-terminal fragment polypeptide showing THREADER secondary-structure predictions and functional subdomains. The region boxed by a solid line corresponds to the recombinant $K_V1.1$ N-terminal fragment polypeptide (amino acids 14-162). Residues with predicted secondary structure are labelled as H (α-helix), E (β-strand) or C (coil). Functional subdomains A,B and C are boxed separately with dashed lines and labelled. The variable regions V1 and V2 are indicated by labelled solid lines. (b) Hypothesized supersecondary structure of the $K_V1.1$ N-terminal fragment based on computer prediction. β-Strands are shown as arrows labelled $\beta1$-$\beta7$. α-Helices are shown as cylinders labelled $\alpha1$ and $\alpha2$. Numbers denote amino acid position in the primary structure. Proposed structural domains N1 and N2 are shaded and labelled.

3.4. Structure prediction based on amino acid sequence

Initial threading of the $K_V1.1$ N-terminal sequence against the standard fold library was unsuccessful in locating a sufficiently high-scoring model to indicate a good match with one particular protein, but several regions of secondary structure and their respective interactions were predicted with some confidence. Upon expanding the library to include structures related to the top hits, however, chain B of mannose-bi-

nding protein A ($MBpA_B$) [16] appeared as a very strong candidate (4.4 standard deviations from the random average) compared to the original fold sets. Previous experience with THREADER suggests that this is a very significant result, although guidelines for this determination do not take modification of the fold library into account. Moreover, the structure obtained on the basis of $MBpA_B$ is consistent with most of the secondary-structure assignments and contacts between secondary structure elements in the majority of the top threadings. Fig. 5a shows the amino acid sequence of $K_V1.1$ N-terminal fragment (top line) with secondary-structure predicted by the THREADER (bottom line) based on the combination of the structure of $MBpA_B$ and other top threading results. Fig. 5b shows the suggested super-secondary structure indicating those structural elements thought to interact with each other. The overall fold consists of two structural domains, each containing an α-helix and a region of anti-parallel β-sheet.

4. Discussion

Conflicting data has previously been presented regarding the ability of the K_V channel N-terminal fragment to tetramerise. In agreement with a number of previous studies [3,4,6], we have shown that the recombinant $K_V1.1$ N-terminal fragment self-assembles into a tetramer in native conditions.

However, our experiments show that with the non-ionic detergent Triton X-100 present in the solution at 1% v/v – a concentration above its critical micellisation concentration (CMC) – tetramerisation is prevented and the N-terminal fragment remains in monomeric form. A similar result was reported by Babila et al. [7], who suggested that the N-terminal fragment cannot efficiently tetramerise in the absence of the membrane-spanning S1 domain. In their study, 1% Triton X-100 detergent was used in multimerisation analysis. This was presumably because the study also encompassed membrane-spanning regions of the channel protein, which require detergent presence for solubility. Our results suggest that it may be their use of 1% Triton X-100 in subunit assembly experiments which prevented tetramerisation in the cytoplasmic N-terminal fragment, but allowed tetramer formation in the hydrophobic S1 domain, the structure and inter-subunit interactions of which would not be perturbed by the use of detergent. This is in agreement with previous studies on other proteins which show that solubilisation of proteins in buffers containing Triton X-100 in concentrations above its CMC can cause multimer dissociation [17].

Although presence of Triton X-100 prevents tetramer formation of the N-terminal fragment, FTIR spectroscopy indicates that solubilisation of the protein in Triton X-100 (1% v/v) does not alter its secondary structure content. Secondary structure content predictions from FTIR and CD spectroscopy agreed very well, giving values of 20–25% α-helix, 20–25% β-sheet, 20% turns and 30–40% random coil. Van 't Hoff enthalpy calculations show that the N-terminal fragment in aqueous solution (tetramer) has four times the unfolding enthalpy of the Triton X-100-solubilised form (monomer). This four-fold enthalpy difference further supports the ability of the N-terminal fragment to tetramerise in the absence of Triton X-100 and its inability to tetramerise in the presence of Triton X-100. This result demonstrates that the presence of 1% Triton-100 disrupts self-assembly of the recombinant $K_V1.1$ N-terminal fragment even when the protein is at the elevated concentration of 50 mg/ml, and validates the comparisons drawn between spectroscopic data and results from the sucrose gradient analysis (performed using a protein concentration of 1 mg/ml).

The relatively rapid hydrogen/deuterium exchange in the tetrameric N-terminal fragment indicates that it adopts a tertiary structure which allows a high degree of solvent accessibility [18,19]. In contrast, in the detergent-solubilised monomeric form, the slower hydrogen/deuterium exchange indicates a tertiary structure with a lower degree of solvent accessibility [18,19]. One interpretation of this result is that tetramerisation of the recombinant $K_V1.1$ N-terminal fragment occurs via the interaction of hydrophobic surfaces, allowing the exposure of water soluble residues with a resulting high degree of solvent accessibility. When solubilised in detergent, however, these interactions between hydrophobic surfaces are disrupted, with a consequent reduction in solvent accessibility of water-soluble residues.

The midpoint temperature of hydrogen/deuterium exchange of the monomeric N-terminal fragment was 41.6 ± 0.8°C, significantly lower than the midpoint

temperatures of unfolding and aggregation for this protein (45–50°C), indicating that the exchange effect here is due to heat-induced changes in tertiary structure and not secondary structure [8]. Enhanced exchange upon heating can also be caused by increased kinetic energy of the NH bonds without structural change, but the sigmoidal decrease in intensity of the amide II band probably rules out this possibility, as the increased energy effect on its own would result in a more gradual temperature dependence [8].

The possibility of the slower hydrogen/deuterium exchange observed for the monomeric N-terminal fragment solubilised using Triton X-100 being due to obscuring of residues by partitioning of the protein into Triton X-100 micelles can be discounted based on previous observations. In the study by Babila and co-workers [7] Triton X-100 (1%, v/v) was used to solubilise the $K_V1.1$ N-terminal domain for sucrose gradient analysis. The resulting calculated sedimentation coefficient and partial specific volume of the N-terminal domain protein indicated that it does not complex with Triton X-100, thus ruling out the possibility that partitioning of the protein into the detergent is responsible for the observed reduction in hydrogen-deuterium exchange observed in the current study.

We have shown that presence of Triton X-100 micelles disrupts both tetramer formation and the tertiary structure of the protein. These two phenomena may be linked, with multimerisation being prevented by disruption of the stereo-specific alignment of residues on neighbouring subunits necessary for self-assembly. Alternatively, detergent presence may directly disrupt the hydrogen bonding and/or hydrophobic interactions necessary for tetramer formation by virtue of its own hydrophobicity.

We have proposed an overall model of $K_V1.1$ N-terminal fragment using the THREADER program (see Fig. 5). The proportions of secondary structure assigned by the THREADER program (19% α-helix, 28% β-sheet and 53% coil or turn structures) compare well with the figures predicted from spectroscopic data of 20–25% α-helix, 20–25% β-sheet and 50–60% coil and turn structures and this adds confidence to the fold predicted using THREADER. Furthermore THREADER predicts that all the regions of β-sheet in the $K_V1.1$ N-terminal fragment are in an anti-parallel conformation, and this is in accord with our spectroscopic results which also indicate that the β-structures in the fragment form anti-parallel β-sheets. The overall fold appears to consist of two structural domains, N1 and N2, each containing one α-helix ($\alpha1$ and $\alpha2$ respectively). These helices lie at 90°C to each other. The N1 domain contains the N- and C-terminal ends, (β-strands $\beta1$ and $\beta7$, respectively) aligned parallel to $\alpha1$ and to the smaller $\beta2$ region. (Fig. 5b). The N2 domain comprises four regions of β-strand arranged into an anti-parallel β-sheet perpendicular to $\alpha2$.

As mentioned earlier, the N-terminal fragment has previously been conceptually divided into three subdomains on the basis of conservation of amino acids in potassium channels (see Fig. 5a). These subdomains (A–C) together with variable regions V1 and V2 collectively comprise the T1 (tetramerisation) domain. Subdomains A and C lie within the N1 domain whilst the N2 domain is essentially the B subdomain capped by the V1 and V2 regions. The conserved subdomain A is known to be responsible for the incompatibility which prevents *Shaker* α-subunits from heteromultimerising with, for example, *Shaw* channel α-subunits [4]. The large proportion of ordered structure predicted for this subdomain may reflect a specific fold important for subunit compatibility. Subdomains A and B are important for the organization of *Shaker* α-subunits into homomultimers [4]. Our model places subdomain A in the N1 and subdomain B in the N2 domain. This separation might be important in the proposed functions of the N-terminal region.

No role has as yet been ascribed to the C subdomain; it may be limited to contributing to the overall fold shape by interacting with residues in subdomain A to bring chain termini together.

This study constitutes the first reported structural analysis of a recombinant K_V channel protein domain. We have shown that the application of low-resolution experimental techniques (CD and FTIR spectroscopy) combined with computational methods (global analysis and structural prediction) to a single protein domain can give significant structural information and an insight into the proposed molecular mechanisms of domains functions.

Acknowledgements

We would like to thank Dr. Giuliano Siligardi at the National Chiroptical Spectroscopy Facility (EPSRC), King's College, Manresa Road, London, for the circular dichroism measurements. G.W.A. is supported by a studentship from BBSRC. We gratefully acknowledge the financial support of the Peter Samuel Royal Free Fund.

References

[1] M. Li, Y.N. Jan, L.Y. Jan, Science 257 (1992) 1225–1230.
[2] A. Baumann, A. Grupe, A. Ackermann, O. Pongs, EMBO J. 7, 8 (1988) 2457–2463.
[3] N.V. Shen, X. Chen, M.M. Boyer, P.J. Pfaffinger, Neuron 11 (1993) 67–76.
[4] N.V. Shen, P.J. Pfaffinger, Neuron 14 (1995) 625–633.
[5] J. Xu, W. Yu, Y.N. Jan, L.Y. Jan, M. Li, J. Biol. Chem. 270, 42 (1995) 24761–24768.
[6] P.J. Pfaffinger, D. DeRubeis, J. Biol. Chem. 270, 48 (1995) 28595–28600.
[7] T. Babila, A. Muscucci, H. Wang, F.E. Weaver, G. Koren, Neuron 12 (1994) 67–76.
[8] I.H.M. Van Stokkum, H. Linsdell, J.H. Hadden, P.I. Haris, D. Chapman, M. Bloemendal, Biochemistry 34 (1995) 10508–10518.
[9] G.W. Abbott, E.A.J. Mercer, M. Wolters, S. Sewing, O. Pongs, S.K.S. Srai, Biochem. Soc. Trans. 23 (1995) 479S.
[10] R.G. Martin, B.N. Ames, J. Biol. Chem. 236, 5 (1961) 1372–1379.
[11] R. Pribif, I.H.M. Van Stokkum, D. Chapman, P.I. Haris, M. Bloemendal, Anal. Biochem. 214 (1993) 366–378.
[12] J.M. Hadden, M. Bloemendal, P.I. Haris, I.H.M. Van Stokkum, D. Chapman, S.K.S. Srai, FEBS Lett. 350 (1994) 235–239.
[13] I.H.M. Van Stokkum, H.J.W. Spoelder, M. Bloemendal, R. Van Grondelle, F.C.A. Groen, Anal. Biochem. 191 (1990) 110–118.
[14] D.T. Jones, W.R. Taylor, J.M. Thornton, Nature 358 (1992) 86–89.
[15] W.F. Maddams, M.J. Southon, Spectrochim. Acta 38A (1982) 459–466.
[16] W.I. Weis, R. Kahn, R. Fourme, K. Drickamer, W.A. Hendrickson, Science 254 (1991) 1608–1615.
[17] A. Shaw, P.A.G. Fortes, C.D. Stout, V.D. Vacquier, J. Cell Biol. 130, 5 (1995) 1117–1125.
[18] P.I. Haris, D.C. Lee, D. Chapman, Biochim. Biophys. Acta 874 (1986) 255–265.
[19] J.M. Olinger, D.M. Hill, R.J. Jakobsen, R.S. Brody, Biochim. Biophys. Acta 869 (1986) 89–98.